Testing for fault activity at Yucca Mountain, Nevada, using independent GPS results from the BARGEN network

Emma M. Hill[1,2] and Geoffrey Blewitt[1]

Received 24 February 2006; revised 24 May 2006; accepted 1 June 2006; published 19 July 2006.

[1] Data from BARGEN GPS stations around Yucca Mountain (YM) have been independently processed using GIPSY-OASIS and GAMIT/GLOBK. The RMS velocity differences between these solutions is 0.06 mm/yr (east component) and 0.10 mm/yr (north), indicating an ability to resolve tectonic signals >0.3 mm/yr with high confidence. Inversion of GPS station velocities for Eastern California Shear Zone (ECSZ) fault parameters produces an unreasonably deep locking depth of ~30 km for the Death Valley-Furnace Creek fault system, contradicting seismological evidence. The GPS cluster locally west of YM observes a strain rate of 17.0 ± 1.8 ns/yr, marginally higher than our ECSZ model predicts (13.9 ± 0.7 ns/yr). Significantly, the cluster to the east observes 22.3 ± 2.1 ns/yr, which is 6.2σ higher than the model (8.6 ± 0.7 ns/yr), suggesting that additional sources of strain more local to YM (<30 km) are currently active, collectively accumulating >0.7 mm/yr. **Citation:** Hill, E. M., and G. Blewitt (2006), Testing for fault activity at Yucca Mountain, Nevada, using independent GPS results from the BARGEN network, *Geophys. Res. Lett.*, *33*, L14302, doi:10.1029/2006GL026140.

1. Introduction

[2] To assist with hazard planning for the Yucca Mountain (YM) nuclear waste repository, the United States Department of Energy has funded the installation and monitoring of a dense, continuous GPS network in the YM region, southern Nevada. An explicit design feature was that the GPS data would be processed independently by two different groups using different software packages and processing models, followed by independent analysis and interpretation. Rather than follow a validation exercise, here we use the differences in station velocities between these independent analyses to estimate the level of systematic "processing noise" as part of our error model, which we then use to test the significance of hypothetical fault activity local to YM. These tests are important because *Wernicke et al.* [2004] claimed that strain rates at YM were higher than geologic predictions. Our independent analysis uses a much longer GPS data set that allows us to quantify the strain rates across subsets of the network with higher spatial resolution to detect possible local sources of deformation.

[3] YM is located ~40 km to the east of the Eastern California Shear Zone (ECSZ), a ~100-km wide zone of right-lateral strike-slip faulting. At the latitude of YM, the most important ECSZ faults are the Owens Valley (OV), Panamint Valley–Hunter Mountain (PV-HM) and Death Valley–Furnace Creek (DV-FC) fault systems (Figure 1). There have been some discrepancies between estimated slip rates for these faults. Some studies have allocated higher slip rates to the west [*McClusky et al.*, 2001; *Gan et al.*, 2000], some to the east [*Dixon et al.*, 2003; *Hearn and Humphreys*, 1998], while others have divided the deformation evenly across the ECSZ [*Bennett et al.*, 2003]. This might reflect the difficulty geodesists face in estimating slip rates from a limited sample of stations. Alternatively, it could reflect the effect of earthquake cycle on measured slip rates [*Dixon et al.*, 2003], or perhaps postseismic relaxation from large 19th and 20th century earthquakes in the region.

[4] YM itself is cut by a number of N-S trending faults, with primarily normal offsets. Estimated geologic slip rates here are extremely low, at 0.01–0.02 mm/yr [*Simonds et al.*, 1995]. The Bare Mountain range-front fault lies W of YM (Figure 2), also with low geologic slip rates of 0.02–0.20 mm/yr [*Wernicke et al.*, 1998]. The ENE-trending Rock Valley fault zone (RVFZ), located SE of YM (Figure 2), is a ~5 km wide and ~32 km long zone of ENE-striking left-lateral and normal faults, with estimated geologic slip rates of 0.02–0.089 mm/yr [*O'Leary*, 2000]. The 1992 M_L5.6 Little Skull Mountain earthquake occurred on a fault adjacent to the RVFZ [*Smith et al.*, 2001], ~20 km to the SE of YM (Figure 2).

[5] A number of studies have examined the effect of the ECSZ on the strain field at YM, also with some discrepancy between their results. Initially, *Wernicke et al.* [1998] had used campaign GPS measurements to estimate an extensional strain rate of 50 ± 9 ns/yr (where 1 ns ≡ 10^{-9}) along a sampled orientation of N65°W. In contrast, *Savage et al.* [1999] concluded that their own measurements of strain at YM at that time (23 ± 10 ns/yr) could be explained (within the errors) by their models of deformation across the ECSZ (10–14 ns/yr). Using continuous GPS data from the BARGEN network, *Wernicke et al.* [2004] estimated a strain rate of 20 ± 2 ns/yr of N20°W right-lateral shear. They concluded that this was difficult to explain using models of DV-FC alone, proposing that a local fault at YM bearing ~0.9 mm/yr of right-lateral strike-slip would explain their results. It is possible that the high strain rate initially measured by *Wernicke et al.* [1998] was caused by

[1]Nevada Bureau of Mines and Geology, University of Nevada, Reno, Nevada, USA.
[2]Now at Harvard-Smithsonian Center for Astrophysics, Cambridge, Massachusetts, USA.

0094-8276/06/2006GL026140$05.00

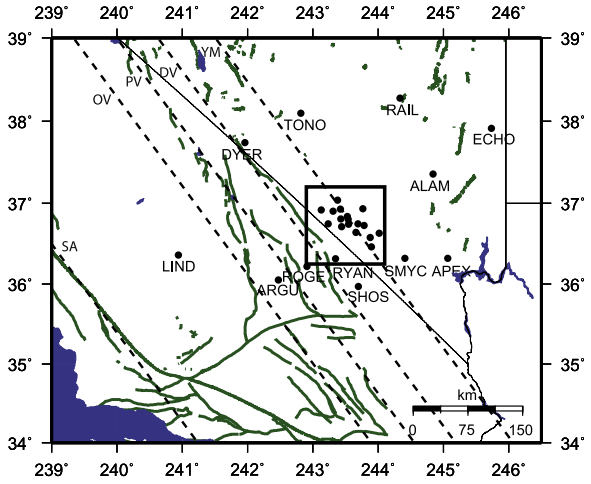

Figure 1. Tectonic setting of Yucca Mountain (YM), showing BARGEN GPS stations (solid circles), Quaternary faults (solid lines) and approximate estimated locations of model faults (dashed lines): San Andreas (SA), Owens Valley (OV), Panamint Valley – Hunter Mountain (PV-HM), Death Valley – Furnace Creek (DV-FC) and local fault at Yucca Mountain (YM). The box outlines the area shown in Figure 2.

postseismic deformation after the 1992 Little Skull Mountain earthquake [*Wernicke et al.*, 2004].

2. GPS Processing

[6] *Wernicke et al.* [2004] processed the GPS data using the GAMIT/GLOBK (GAMIT) software, which implements the double difference technique. In contrast, we processed the data independently using precise point positioning by the GIPSY-OASIS II (GIPSY) software [*Zumberge et al.*, 1997] from the Jet Propulsion Laboratory (JPL). In both cases, ambiguity resolution was applied. The GIPSY processing was carried out automatically using JPL's default settings, with no manual intervention. GIPSY solutions were transformed into the ITRF2000 reference frame using 7 parameters each day determined by JPL. Euler vector rotations then transformed the velocities into a North-American-plate fixed reference frame [*SNARF Working Group*, 2005] and also into a Pacific frame [*DeMets et al.*, 1994]. Spatial filtering was applied to minimize common-mode signals [*Wdowinski et al.*, 1997].

[7] By May 1999 an additional 30 stations had been added south of the existing BARGEN network ("SBAR", Figure 1) of which 16 stations formed a dense network local to YM ("YM network", Figure 2). In late 1999 there were a number of offsets recorded in the SBAR time series from the 1999 M_w7.1 Hector Mine earthquake and from hardware changes within the network. The earthquake offset was estimated and removed. The YM network had radome changes in August 1999, but the far-field SBAR network had changes several months later. This caused a "box-car"-type offset in the vertical time series that, if not taken into account, gave the artificial impression of a local YM uplift relative to the far-field. These offsets were avoided simply by removing all data from the solution that fell between the first and last radome changes. We find solutions containing data from May 1999, with estimation and removal of the 1999 offsets, are not significantly different to solutions using only data from after the final offset, from 15 January 2000. Hence we consider the effective data span of this study and of *Wernicke et al.* [2004] to begin on this date.

[8] We use two GIPSY solutions in this paper: (1) for scientific interpretation, we use a 5.7-yr span of data from January 2000 to September 2005; and (2) for purposes of quantifying differences with the GAMIT solution [*Wernicke et al.*, 2004] we use a 3.8-yr effective span of data from May 1999 to October 2003, with offsets modeled and removed.

3. Station Velocities and Strain Rates

[9] The normalized chi-square from fitting a constant velocity model to daily station position time series is 0.9, indicating that formal errors from GIPSY realistically model the precision. The RMS of relative velocity differences between the GIPSY and GAMIT results (Figure 2) for the 3.8-yr solution is 0.06 mm/yr for the east component, and 0.10 mm/yr for the north. We use this result to define a systematic "processing error," which we add to the GIPSY formal errors to obtain total errors. In doing so we model the level of processing-related velocity error as a constant level of error in cumulative displacement divided by the time span of the data. Applying this procedure to the new 5.7-yr solution effectively scales the GIPSY errors by a factor of ~4, producing "total" errors (1 s.d.) in 2-D relative velocity at the level of 0.08 mm/yr (equivalent to ~0.5 mm

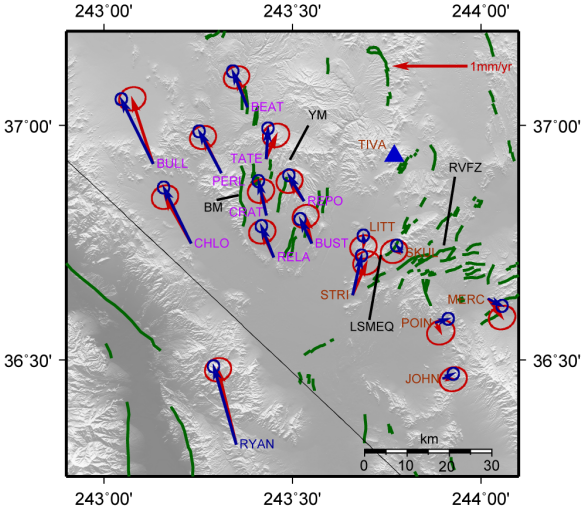

Figure 2. Comparison of velocities from GIPSY at 5.7 yr (this study, blue) and from GAMIT published by *Wernicke et al.* [2004] at 3.8 yr (red). Velocity estimates are plotted as baselines relative to station TIVA (blue triangle) in a North-American-plate fixed reference frame. Error ellipses are 95% confidence based on scaled standard deviations. Also marked are the locations of Yucca Mountain (YM), the Bare Mountain range fault (BM), the Rock Valley Fault Zone (RVFZ), and the location of the 1999 Little Skull Mountain earthquake (LSMEQ). All stations except RYAN define the local YM network. Stations in the western cluster are labeled in purple, and stations in the eastern cluster labeled in orange.

Table 1. Results of Inversions of the GPS Results for Slip Rate (S) and Locking Depth (D) for the San Andreas (SA), Owens Valley (OV), Panamint Valley-Hunter Mountain (PV-HM), Death Valley-Furnace Creek (DV-FC) Fault Systems, With and Without a Model Fault at Yucca Mountain

	No Local Model Fault		Local Fault Included	
Fault	D, km	S, mm/yr	D, km	S, mm/yr
SA	16.3 ± 3.8	30.7 ± 0.4	10.2 ± 3.8	30.6 ± 0.4
OV	9.2 ± 4.0	2.2 ± 0.5	7.3 ± 4.0	3.1 ± 0.6
PV-HM	15.6 ± 3.8	3.7 ± 0.9	8.6 ± 3.7	4.5 ± 0.9
DV-FC	29.2 ± 1.5	5.9 ± 0.7	7.5 ± 2.7	3.0 ± 0.5
YM	N/A	N/A	12.8 ± 2.3	1.0 ± 0.1

cumulative displacement over 5.7 yr). These total errors are then propagated into fault models and strain rate calculations. The errors compare with a velocity error of 0.15 mm/yr for the YM network predicted by *Davis et al.* [2003] using a shorter data span.

[10] When plotted relative to the site TIVA (E of YM), the horizontal velocities generally trend NNW and increase in magnitude from east to west (Figure 2). The magnitude of the velocity contrast across the network, from TIVA to BULL, is 0.97 ± 0.08 mm/yr (over a distance of 57 km). The directions of POIN, MERC, JOHN, and STRI appear to be different compared to the other stations. These stations are located SE of YM, around the RVFZ. The direction of station TATE (NW of YM) is anomalously eastward relative to surrounding stations. Much of the essential details of the pattern of station velocities are the same in the 5.7-yr GIPSY solution and 3.8-yr GAMIT solution, suggesting signals of a tectonic origin. While we do not interpret the vertical component here, the RMS scatter of vertical velocities about the mean is 0.23 mm/yr.

[11] Strain rates were estimated empirically for (1) all stations in the YM network, (2) 9 stations at and to the west of YM (the western cluster), and (3) 7 stations to the east of YM (the eastern cluster). These clusters are identified in Figure 2 (and all clusters are listed in the auxiliary material[1].) The average engineering shear strain rate for all stations is 18.5 ± 1.0 ns/yr, oriented N21 ± 1°W. This agrees statistically with *Wernicke et al.* [2004], but our value is smaller and more precise. However, we find the strain rate is not constant across the YM network. The average shear strain for the western cluster is 17.0 ± 1.8 ns/yr oriented N22 ± 2°W, while for the eastern cluster it is higher at 22.3 ± 2.1 ns/yr oriented N13 ± 2°W. This is unexpected considering that the eastern cluster is further from the ECSZ. This rate decreases to 14.3 ± 2.5 ns/yr if station STRI is omitted from the estimation, suggesting that deformation may be occurring close to the RVFZ.

4. Fault Modeling

[12] An elastic dislocation model [*Savage and Burford*, 1973] was used to invert for location, slip rate and locking depth of faults that could influence the deformation field at YM. We modified this (flat-earth) model, to account for the far-field kinematic boundary conditions implied by rigid plate tectonics on a sphere [e.g., *Murray and Segall*, 2001], by substituting horizontal velocities in the equation with rotation (Euler) vectors. The GPS results were input to the inversion as rotation rates relative to a stable Pacific (PA) plate, which enabled us to avoid the uncertainty associated with stable North America (NA) reference frames and zero model velocity. The model profile sums over each fault from west to east:

$$\Omega_g = \sum_{f=1}^{N} \left[\frac{\omega_f}{\pi} \arctan\left(\frac{r_f - r_g}{D_f} \right) + \frac{\omega_f}{2} \right] \quad (1)$$

where Ω_g is total rotation at station g as a result of deformation across all model faults; r_g is distance from the GPS station to the NA-PA Euler pole; r_f is the distance from each fault f to the NA-PA Euler pole; D_f is fault locking depth; and w_f is fault slip rate expressed as a rotation.

[13] The fault model and GPS data (all stations in Figure 1 except those north of latitude 37.5°) were input to a constrained, weighted, least-squares inversion for fault parameters. The fit of the model profile to the GPS profile was determined by calculating the RMS of the velocity differences. Faults used in the initial inversion were the SA, OV, PV-HM and DV-FC fault systems (Figure 1). These were modeled to follow a circle around the NA-PA Euler pole. A second inversion included a hypothetical model fault within the local YM network. In contrast, *Wernicke et al.* [2004] used only DV-FC in a forward model of the data, using a NA-fixed reference frame.

[14] Table 1 and Figure 3 show the results of these inversions. Although the local model fault is estimated to run roughly through YM itself, the data would also be consistent with fault activity that is distributed between several of the mapped fault traces near YM. The current GPS station density, however, does not allow resolution of the local fault location to better than ~15 km. The local model fault, therefore, is simply representative of the integral of slip rates distributed across the local network.

[15] RMS velocity difference between model and GPS results reduces from 0.22 mm/yr to 0.18 mm/yr when a model fault local to YM is included. Moreover, the inversion with no local model fault estimates a locking depth for DV-FC of 29.2 ± 1.5 km, due to the inversion fitting the model through the relatively steep gradient in the GPS profile across the local YM network. This depth is unreasonable because ~99% of hypocentral depths recorded for the area have been 16 km (http://quake.geo.berkeley.edu/anss/catalog-search.html). The estimated locking depth reduces to within the seismogenic zone (7.5 ± 2.7 km) when a local fault is included. The estimated slip rate for the local model fault is 1.0 ± 0.1 mm/yr, from which we infer that >0.7 mm/yr of relative motion is likely to be accommodated by sources local to YM.

[16] Model strain rates for the YM network were estimated from model station velocities predicted by the estimated fault parameters. Contributions from the SA, OV, HM-PV and DV-FC were all included, using the inversion with and without a local model fault. Estimated model shear strain for the western cluster of stations, with no local fault, is 13.9 ± 0.7 ns/yr, which is 1.6σ lower than the empirical GPS estimate of 17.0 ± 1.8 ns/yr (formal errors for the

[1] Auxiliary material data sets are available at ftp://ftp.agu.org/apend/gl/2006gl026140. Other auxiliary material files are in the HTML.

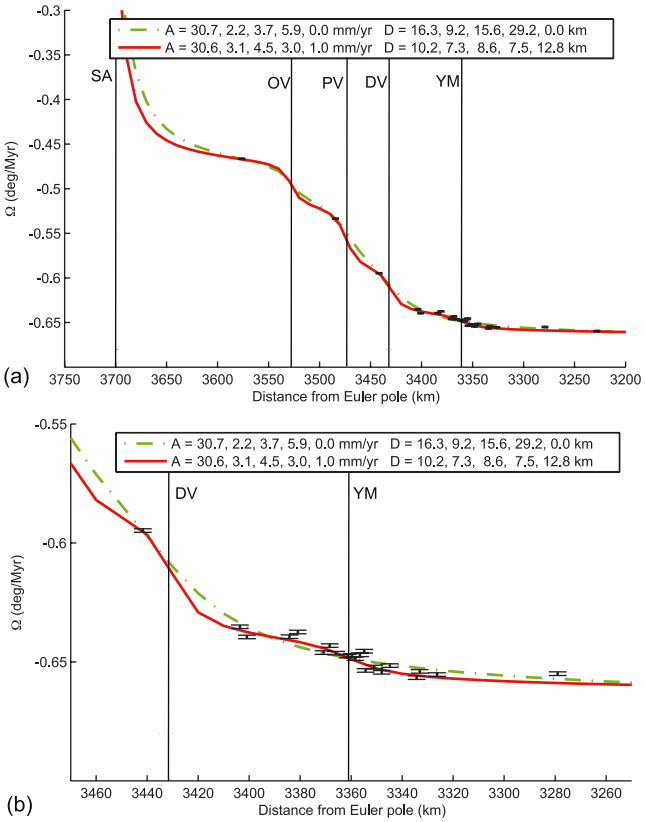

Figure 3. Model profiles produced using the results of an inversion for San Andreas (SA), Owens Valley (OV), Panamint Valley-Hunter Mountain (PV-HM) and Death Valley-Furnace Creek (DV) fault parameters, with (solid line) and without (dashed line) a local model fault at Yucca Mountain (YM). Profiles and GPS results are plotted as rotation rates about the North American Euler pole, in a Pacific plate fixed reference frame, with 1σ error bars on the GPS results. (b) A close-up of the YM local network.

model strain rates do not account for systematic errors due to simplifications of the model). Estimated model shear for the eastern cluster, however, is 8.6 ± 0.7 ns/yr, which is significantly lower (6.2σ) than the 22.3 ± 2.1 ns/yr estimated from the GPS results. The model strain rate for all stations in the YM network (11.3 ± 0.4 ns/yr) is also significantly lower (6.7σ) than the GPS estimate (18.5 ± 1.0 ns/yr).

[17] Including a local fault produces a model strain rate for the western cluster (20.0 ± 0.9 ns/yr) that agrees with the GPS result to 1.5σ. The model strain rate for all stations in the YM network (17.7 ± 0.6 ns/yr) also agrees with the GPS result. The model strain rate for the eastern cluster is increased to 13.8 ± 1.0 ns/yr, although this is still significantly lower (3.7σ) than the GPS result, unless station STRI is excluded, in which case the agreement is excellent.

5. Discussion

[18] Our results indicate that the GPS-measured deformation field at YM cannot be explained by models of the ECSZ faults alone, and that the models appear to require deformation across a local structure within the YM area, thus supporting the hypothesis of *Wernicke et al.* [2004]. Four pieces of evidence support this: (1) the average strain rate across the YM network (18.5 ± 1.0 ns/yr) cannot be explained by models of the ECSZ, even when the ECSZ fault models are estimated by the GPS data themselves (11.3 ± 0.4 ns/yr); (2) in the absence of model faults local to YM, the estimated locking depth of the DV-FC fault system is too deep (∼30 km) as compared with seismological estimates (∼16 km); (3) far-field deformation from ECSZ faults alone predicts decreasing strain rates going from west to east, but observations show otherwise, and the discrepancy between observed and modeled strain becomes significantly worse east of YM (a 6σ effect); and (4) estimation of fault parameters local to YM indicates that the slip rate is likely to be >0.7 mm/yr, where this can also be interpreted as a cumulative slip rate across several active structures, or as an approximate sum estimate of other unmodeled sources of deformation in the area.

[19] We note that the model fault geometries are a simple approximation of the actual fault traces. Particularly, the DV-FC fault system changes orientation at the approximate location of YM and the model fault does not take this into account. However, no matter how refined we may make the models, they will never predict increasing strain rates going east of YM unless a local fault is included.

[20] Although the strain rate for the eastern YM cluster could be caused by NW-trending, right-lateral, strike-slip faults across the local YM network, an alternative hypothesis is that the source of the measured strain is left-lateral strike-slip deformation across the NE-trending RVFZ. Several new YM network stations installed in late 2005 will eventually help to test this possibility. The fact that strain rates for the eastern cluster decrease when station STRI is removed may also indicate the location of deformation.

[21] Another possible unmodeled source of strain is postseismic relaxation from a number of earthquakes, though it remains to be seen if this explains the strain rates observed at YM today. Postseismic effects might eventually be detected as accelerations in longer time series. With more stations, postseismic relaxation of a specific earthquake might be recognized by its characteristic spatial "fingerprint" in strain rate, as it differs from the pattern of interseismic strain accumulation.

[22] **Acknowledgments.** This research was supported by DOE contract FC-08-98NV12081. We thank D. Argus and an anonymous reviewer for constructive comments.

References

Bennett, R. A., B. P. Wernicke, N. A. Niemi, A. M. Friedrich, and J. L. Davis (2003), Contemporary strain rates in the northern Basin and Range province from GPS data, *Tectonics*, *22*(2), 1008, doi:10.1029/2001TC001355.

Davis, J. L., R. A. Bennett, and B. P. Wernicke (2003), Assessment of GPS velocity accuracy for the Basin and Range Geodetic Network (BARGEN), *Geophys. Res. Lett.*, *30*(7), 1411, doi:10.1029/2003GL016961.

DeMets, C., R. G. Gordon, D. F. Argus, and S. Stein (1994), Effect of recent revisions to the geomagnetic reversal time scale on estimates of current plate motions, *Geophys. Res. Lett.*, *21*(20), 2191–2194.

Dixon, T. H., E. Norabuena, and L. Hotaling (2003), Paleoseismology and Global Positioning System: Earthquake-cycle effects and geodetic versus geologic fault slip rates in the Eastern California Shear Zone, *Geology*, *31*(1), 55–58.

Gan, W., J. L. Svarc, J. C. Savage, and W. H. Prescott (2000), Strain accumulation across the Eastern California Shear Zone at latitude 36°30′N, *J. Geophys. Res.*, *105*(B7), 16,229–16,236.

Hearn, E. H., and E. D. Humphreys (1998), Kinematics of the southern Walker Lane Belt and motion of the Sierra Nevada block, California, *J. Geophys. Res.*, *103*(B11), 27,033–27,049.

McClusky, S. C., S. C. Bjornstad, B. H. Hager, R. W. King, B. J. Meade, M. M. Miller, F. C. Monastero, and B. J. Souter (2001), Present day kinematics of the Eastern California Shear Zone from a geodetically constrained block model, *Geophys. Res. Lett.*, *28*(17), 3363–3372.

Murray, M. H., and P. Segall (2001), Modeling broadscale deformation in northern California and Nevada from plate motions and elastic strain accumulation, *Geophys. Res. Lett.*, *28*(22), 3215–4318.

O'Leary, D. (2000), Tectonic significance of the Rock Valley Fault Zone, Nevada test site, in Geologic and Geophysical Characterization Studies of Yucca Mountain, Nevada, A Potential High-Level Radioactive-Waste Repository, edited by J. W. Whitney and W. R. Keefer, *Digital Data Ser. 058*, U.S. Geol. Surv., Denver, Colo.

Savage, J. C., and R. O. Burford (1973), Geodetic determination of relative plate motion in central California, *J. Geophys. Res.*, *78*(5), 832–845.

Savage, J. C., J. L. Svarc, and W. H. Prescott (1999), Strain accumulation at Yucca Mountain, Nevada, 1983–1998, *J. Geophys. Res.*, *104*(B8), 17,627–17,631.

Simonds, F. W., J. W. Whitney, K. F. Fox, A. R. Ramelli, J. C. Yount, M. D. Carr, C. M. Menges, R. P. Dickerson, and R. B. Scott (1995), Map showing fault activity in the Yucca Mountain area, Nye County, Nevada, *U.S. Geol. Surv. Misc. Geol. Invest. Ser. Map I-2520*.

Smith, K. D., J. N. Brune, D. M. de Polo, M. K. Savage, R. Anooshehpoor, and A. F. Sheehan (2001), The 1992 Little Skull Mountain earthquake sequence, southern Nevada test site, *Bull. Seismol. Soc. Am.*, *91*(6), 1595–1606.

SNARF Working Group (2005), Workshops for establishing a stable North American reference frame (SNARF) to enable geophysical and geodetic studies with EarthScope: Annual Report 2004–2005, paper presented at the EarthScope National Meeting, Santa Ana Pueblo, New Mexico, 28 March.

Wdowinski, S., Y. Bock, J. Zhang, P. Fang, and J. Genrich (1997), Southern California permanent GPS geodestic array: Spatial filtering of daily positioning for estimating coseismic and postseismic displacements induced by the 1992 Landers earthquake, *J. Geophys. Res.*, *102*(B8), 18,057–18,070.

Wernicke, B. P., J. L. Davis, R. A. Bennett, P. Elosegui, M. J. Abolins, R. J. Brady, M. A. House, N. A. Niemi, and J. K. Snow (1998), Anomalous strain accumulation in the Yucca Mountain area, Nevada, *Science*, *279*, 2096–2100.

Wernicke, B., J. L. Davis, R. A. Bennett, J. E. Normandeau, A. M. Friedrich, and N. A. Niemi (2004), Tectonic implications of a dense continuous GPS velocity field at Yucca Mountain, Nevada, *J. Geophys. Res.*, *109*(12), B12404, doi:10.1029/2003JB002832.

Zumberge, J. F., M. B. Heflin, D. C. Jefferson, M. M. Watkins, and F. H. Webb (1997), Precise point positioning for the efficient and robust analysis of GPS data from large networks, *J. Geophys. Res.*, *102*(B3), 5005–5017.

G. Blewitt, Nevada Bureau of Mines and Geology, MS 178, University of Nevada, Reno, NV 89557, USA. (gblewitt@unr.edu)

E. M. Hill, Harvard-Smithsonian Center for Astrophysics, 60 Garden Street, MS 42, Cambridge, MA 02138, USA. (ehill@cfa.harvard.edu)